The least-squares line and plane and the analysis of palaeomagnetic data

J. L. Kirschvink *Department of Geological and Geophysical Sciences, Princeton University, Princeton, New Jersey 08544, USA*

Summary. The classic, multivariate technique of principal component analysis can be used to find and estimate the directions of lines and planes of best least-squares fit along the demagnetization path of a palaeomagnetic specimen, thereby replacing vector subtraction, remagnetization circles and difference vector paths with one procedure. Eigenvalues from the analysis are the variance of the data along each principal axis, and provide a relative measure of collinearity or coplanarity which may be used to define a general palaeomagnetic precision index. Demagnetization planes found with principal component analysis may be used in place of difference vector paths for locating Hoffman–Day directions, avoiding unnecessary vector subtraction and intensity truncation steps. Two methods are discussed for jointly estimating an average remanence direction from demagnetization lines and planes.

1 Introduction

The Earth's magnetic field continually changes in polarity, direction, and intensity when viewed through geologic time. After its formation, a rock is exposed to a variety of changing magnetic fields. If at certain times during this history, it is subjected to physical or chemical conditions which alter its mineralogy or magnetic properties, it may completely or partially gain a new magnetic remanence. Typically, this new remanence will form a discrete component parallel to the local geomagnetic field direction and add vectorially to any of the original remanence remaining in the rock. Although it is desirable in most palaeomagnetic studies to find the direction of all these various components, techniques currently in use do not exploit all of the available data (especially intensity). Ideally, analytical methods at both the specimen and sample levels should be based on as much of the original magnetic information as possible, with minimal assumptions. To accomplish this goal, it is necessary to first apply the classic multivariate technique of principal component analysis to collinear and coplanar points along a specimen's demagnetization path. Principal component analysis provides estimates of relative collinearity or coplanarity of the data, as well as directions of best least-squares fit. Next, if groups of lines and planes of specimens from different samples

respectively yield clusters (bipolar with mixed N and R data) and girdles of directions on a stereonet which indicate a common magnetic component, all of the directions should be combined into a joint estimate for the average remanence. Techniques for both of these are discussed and developed in Sections 2 to 6, and applied to palaeomagnetic examples in Section 7.

Although principal component analysis is based partly on least-squares minimization, it should not be confused with the exponential least-squares modelling technique of Stupavsky & Symons (1978). Their technique presumes a log-normal grain size-coercivity distribution in space and requires systematic af demagnetization data; when applicable, their exponential models may have greater ability to resolve superimposed components. Many sedimentary rocks, however, do not respond well to af demagnetization, and the magnetic grain-size distributions of freshwater and marine sediments may for example be disturbed by a discrete, single domain spike of biogenic magnetite (Frankel, Blakemore & Wolfe 1979; Kirschvink & Lowenstam 1979). Techniques discussed in this paper are generally applicable to all remagnetization data regardless of demagnetization procedure, magnetic mineralogy, type of remanence or grain-size distribution.

2 Separation of magnetic components

Directions of magnetic components within a rock may be separated by progressively destroying in small increments the natural remanence through heating, af demagnetization, chemical leaching or other demagnetizing procedures; these experiments attempt in part to reverse in the laboratory the mechanisms by which the remanence was gained in nature. The orientation and intensity of the magnetism measured after an incremental demagnetization experiment constitutes a magnetic vector, the 'tip' of which forms a point in magnetic three-space; the set of all such points produced during progressive demagnetization defines the demagnetization path for the specimen. Conversely, a point in magnetic three-space represents a vector pointing from the origin to it. Ordered points along these paths conceptually fall into three geometric groups: lines, planes and three-dimensional curves. A series of points which are collinear usually indicate the progressive removal of one magnetic component; the direction of the line containing them is, of course, parallel to the discrete magnetic vector that was removed. Coplanar points are likewise found when two discrete magnetic components are simultaneously removed in differing ratios; this plane is best described by its pole (perpendicular direction). It should be emphasized that the direction found for a line on a demagnetization path is an estimate of where the remanence *is*, while a pole to a demagnetization plane is an estimate of where the remanence *is not*. Both are of use in palaeomagnetic studies as will be discussed in Sections 5 and 6. The third category, a three-dimensional curve, is produced by the simultaneous, progressive removal of more than two discrete magnetic components. These three geometrical groups may be encountered individually, or together in any order along the demagnetization path of a palaeomagnetic specimen, and it is important in nearly all such studies to recognize the lines and planes within the data and estimate their direction.

Many techniques have been proposed and are currently used in palaeomagnetic studies to locate and estimate the direction of collinear and coplanar points along a demagnetization path. The most popular include the best demagnetization step, stable end point, orthogonal projection, vector subtraction, remagnetization circles and difference vector paths (for example Collinson, Creer & Runcorn 1967; Zijderveld 1967; Khramov 1958; Halls 1976, 1978; Hoffman & Day 1978). The success of these palaeomagnetic techniques is generally unquestioned; they often yield reasonably accurate estimates of the desired magnetic

directions. However, all of these techniques either use only one or two of the data points (such as vector subtraction) or exclude a major part such as the intensity (remagnetization circles and difference vector paths). The classic multivariate technique of principal component analysis (Pearson 1901; Hotelling 1933) was developed to handle this type of data without such unnecessary exclusion, but it has not been used in progressive demagnetization studies. Because recent technological developments have substantially reduced the effort required to progressively demagnetize and measure a rock specimen (Molyneux 1971; Goree & Fuller 1976), large amounts of data are rapidly becoming available. It therefore seems timely to replace the graphical and vector-subtraction techniques currently in use with the analytic rigor of principal component analysis. For lines and planes, this method provides directions of best least-squares fit to the data as well as a measure of their collinearity or coplanarity.

3 Principal component analysis

Principal component analysis is simply a linear transformation of the orthogonal coordinate axes to a new orthogonal reference frame that corresponds to the geometry of the data set. The origin in the new system corresponds to the 'centre of mass', while the new axes are positioned by least-squares to best fit the data. Each axis in the new reference system has associated with it a measure of the variance (σ^2) about the mean in that particular direction; two of the axes are positioned to correspond to the maximum and minimum direction of variance, while the other (in the three-dimensional case) is intermediate. Through the use of Lagrange multipliers, it can be shown that the principal axes parallel the eigenvectors of the matrix of sums of squares and products,

$$H = \begin{bmatrix} \Sigma(x_i - \bar{x})^2 & \Sigma(x_i - \bar{x})(y_i - \bar{y})^2 & \Sigma(x_i - \bar{x})(z_i - \bar{z}) \\ \Sigma(x_i - \bar{x})(y_i - \bar{y}) & \Sigma(y_i - \bar{y})^2 & \Sigma(y_i - \bar{y})(z_i - \bar{z}) \\ \Sigma(x_i - \bar{x})(z_i - \bar{z}) & \Sigma(y_i - \bar{y})(z_i - \bar{z}) & \Sigma(z_i - \bar{z})^2 \end{bmatrix} \quad (1)$$

where $P_i = [x_i, y_i, z_i]$, $i = 1, N$ are the N data points in the old coordinate system and $U = [\bar{x}, \bar{y}, \bar{z}]$ is the position of the origin for the new system. Eigenvalues ($\lambda_{max}, \lambda_{int}, \lambda_{min}$) associated with each eigenvector are the variance of the data along the new axes. If the points all lie precisely along a line, for example, all of the variance is parallel to it. One principal component completely represents the data, and the dimensionality of the total system may be reduced. In this case two eigenvalues will be zero while the third is large, one eigenvector will parallel the line and the other two will be at arbitrary right angles to it. Similarly, there is no variance perpendicular to a plane which contains all of the data; the pole to this plane is the eigenvector associated with the zero variance.

This mathematical procedure is equivalent to finding the lines and planes of best least-squares fit as derived by Schomaker *et al.* (1958) and Blow (1960). If the data are treated as point masses, the mathematics are equivalent to finding the principal axes of inertia about the point U. Note that if U is taken as some point other than the centre of mass, the lines and planes will still be constrained to pass through it while at the same time minimizing the sum of squared deviations. Matrix H is also equivalent to Watson's (1960) matrix of sums of squares and products if each data point, P_i, is truncated to unit distance from the origin and the point U is taken as $[0, 0, 0]$. In this form H serves as the basis for Dimroth–Watson and Bingham spherical statistics (Watson 1960, 1965, 1966; Dimroth 1963; Bingham 1964, 1974). Most computing centres have standard software programs for computing eigenvectors and eigenvalues from symmetric matrices, the IBM Scientific Subroutine Package (SSP) routine EIGEN is one such program.

4 Application to palaeomagnetics

4.1 LOCATION OF LINES AND PLANES

Groups of points which belong to lines and planes along a demagnetization path have been recognized in most palaeomagnetic studies using graphical techniques. Lines are recognized
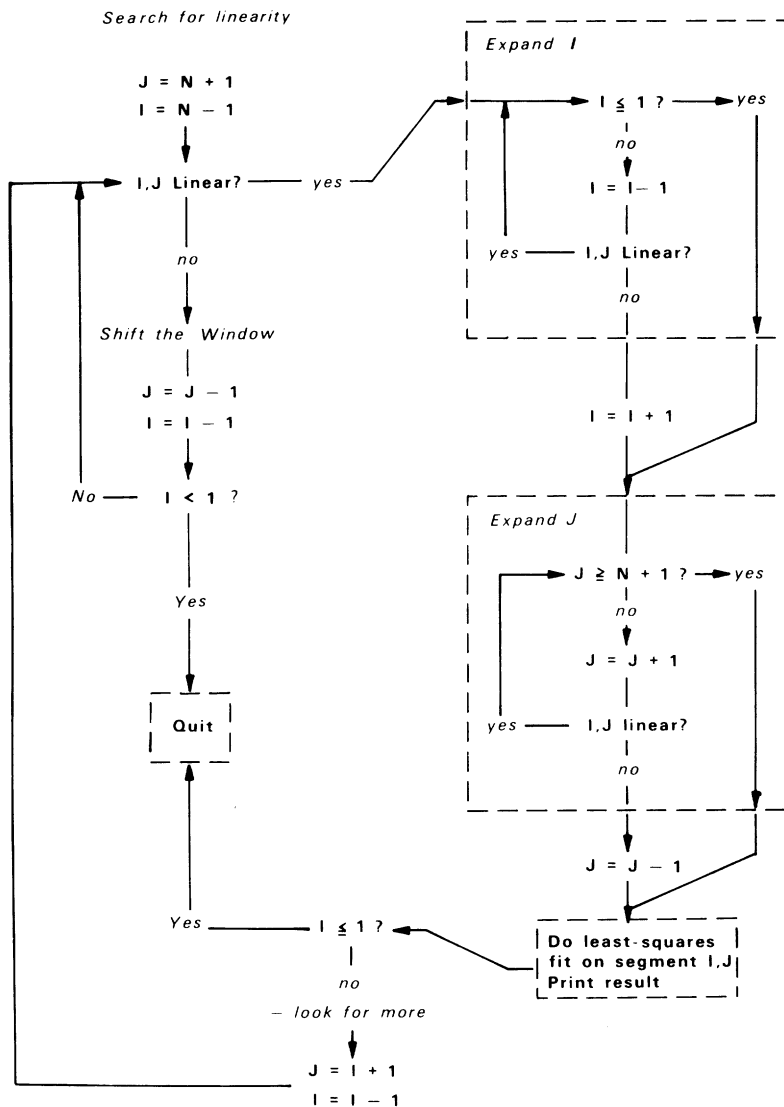

Figure 1. A flow chart for locating collinear and coplanar pieces of the demagnetization path. The N data points are numbered sequentially starting with the NRM, and a search begins by setting the J index on the origin $(0, 0, 0)$ and the index I on the N-1th point. These three points in the first window between I and J are checked for linearity. If they do not fall on a line, the window is moved further down the demagnetization path and again tested. When three collinear points are found, neighbouring points are added until the boundaries of the straight segment are located. The window is then repositioned and the search process repeated until no further linearity remains. The 'I, J linear?' test is positive if the MAD for the points I to J is less than a given value. Data points which lie on a plane may be found by starting with a similar four-point search window.

as straight segments after orthogonal projection (Zijderveld 1967) or as stable endpoint clusters on a stereonet. Planes which pass through the origin can be found by great circle arcs left on a stereonet (Creer 1957; Khramov 1958; Halls 1976, 1978), and planes which do not include the origin have been recognized by great circle paths produced by successive difference vectors (Hoffman & Day 1978). Although reasonably accurate, this eyeball interpretation is not really necessary. Principal component analysis can be used to group a set of points along a demagnetization path into the three categories discussed earlier on the basis of their eigenvalues; $\lambda_{max} \gg \lambda_{int} \gtrsim \lambda_{min} \simeq 0$ implies that the data are grouped on a line, $\lambda_{max} \gtrsim \lambda_{int} \gg \lambda_{min} \simeq 0$ implies a plane, and $\lambda_{max} \gtrsim \lambda_{int} \gtrsim \lambda_{min} \gg 0$ suggests a three-dimensional curve. A simple, easily-computerized procedure which can be used to locate linear or planar groups of points along a demagnetization path is explained on the flow diagram shown in Fig. 1. Once this, a similar algorithm, or an eyeball, has identified groups of collinear or coplanar points, principal component analysis may be used to find the direction of best fit to a line or the pole to a plane. Throughout the rest of this paper, these collinear and coplanar groups of points will be referred to as demagnetization lines or demagnetization planes, respectively.

4.2 CRITERIA FOR DETERMINING LINEARITY OF PLANARITY

A numerical search of the type outlined on Fig. 1 needs a uniform criterion for deciding the linearity or planarity of a group of points. Because the eigenvalues from a principal component analysis are the variance in each principal direction, a simple approach is to ask what the Maximum Angular Deviation (MAD) of the direction would be if the fit along each axis was off by one (or an equal amount of) standard deviation (σ). By analogy with a long rectangular box of dimensions σ_{max}, σ_{int}, σ_{min}, this characteristic angle of equal deviation for a line would be that between the central diagonal and a long edge, or

$$\tan^{-1}(\sqrt{\sigma_{int}^2 + \sigma_{min}^2}/\sigma_{max}),$$

or

$$\tan^{-1}[\sqrt{(\lambda_{int} + \lambda_{min})/\lambda_{max}}].$$

By considering a thin rectangular box with a diagonal plane, the maximum angle of deviation for the pole to a demagnetization plane is similarly found to be

$$\tan^{-1}(\sqrt{\lambda_{min}/\lambda_{int} + \lambda_{min}/\lambda_{max}}). \tag{3}$$

Note that only the relative magnitudes of the three eigenvalues are important. Although these angles are not strict confidence limits, small values respectively indicate collinearity or coplanarity of the data and may be used in a numerical search (Fig. 1). The eigenvalues thus provide a basis for accepting or rejecting data from a particular specimen. Lund & Streletz (1979) have proposed a similar technique involving principal value perturbations. Measurement error and the magnitude of superimposed magnetic components are the only factors which will increase the variance and lead to larger MAD values. Groups of points with values above a specified standard therefore may be omitted from further analysis, leading to the possible exclusion of entire specimens which are found to possess neither collinear nor coplanar points. In this sense, the maximum angle of deviation is a general palaeomagnetic precision index and may serve in place of stability indices used by earlier workers (Tarling & Symons 1967; Ade-Hall 1969; Briden 1972; Symons & Stupavsky 1974; see also the critique by Andel 1970). Unlike other indices, the MAD is purely

geometric and bears little or no relationship to the demagnetization procedure used or to the intensity of the demagnetizing process between measurements. MAD values change little by the addition of new points beyond the stage at which the continuous shape of the demagnetization path is approximated by the data along it. The optimum number of demagnetization steps for a given specimen depends upon its magnetic complexity; three points (including the origin) are the minimum number necessary to check for collinearity, while four are needed to check for coplanarity. For example, each component from a three-component specimen conceivably could be specified by eight measurements plus the origin (nine total points) if their coercivity or blocking temperature spectra did not overlap.

4.3 ANCHORING LINES AND PLANES TO THE ORIGIN

Within whichever error limits are used, if the origin happens to lie on a demagnetization line or plane a slight analytical variation may be substituted for computing the principal direction of best fit. Physically, inclusion of the origin for a line implies that only one component remains in the rock; for a plane only two remain. All others, if there were any, have been removed by demagnetization. The difference in technique arises because the origin is an exact theoretical point on all demagnetization paths. (Completely demagnetized specimens should have no remanence.) In this case, use of the origin instead of the centroid as the point U in equation (1) mathematically forces the line or plane of best fit into agreement with the physical interpretation. The centroid is used for the general case because it is the best available estimate of a point which lies on the line or plane of best fit; in the particular case at hand the origin is theoretically better. An anchored demagnetization line is the least-squares generalization of a stable end-point direction while an anchored plane is the similar generalization of a remagnetization circle.

5 Generalizations of analytical techniques involving demagnetization planes

5.1 COMPARISON OF PLANAR METHODS

Before techniques which have in the past been used for analysis of coplanar data are compared, it seems worthwhile to illustrate interrelationships between the various methods. The solid curve on the top half of Fig. 2 is a schematic drawing of a planar demagnetization path. Arrows which connect the origin of the unit circle to the path are the remanence vectors measured directly after each demagnetization step. A free demagnetization plane in this case would pass through the centroid ($U = \oplus$) and be fit to all known points (NRM, A, B, . . . , F, Origin). The direction of the pole is found by principal component analysis on the original data. An anchored demagnetization plane would use the origin instead of the centroid as point U in equation (1), and be fit to points NRM through F along the demagnetization path. For a remagnetization circle (Creer 1957, 1962; Khramov 1958; Halls 1976, 1978), only the direction of each remanence vector is considered as would be viewed on a stereonet. On Fig. 2, small open squares are drawn around points where the remanence vectors intersect the unit sphere; a plane constrained to pass through the origin is fit to these normalized directions. Finally, the last technique which has been proposed for determining the orientation of these coplanar points is to consider the path of successive difference vectors (Hoffman & Day 1978). On Fig. 2, these coplanar vectors are shown as dashed arrows which sequentially connect adjacent points along the demagnetization path. After regrouping so that they start at the origin as shown on the bottom circle, a new plane passing through the origin can again be fit to the normalized directions shown as the circled
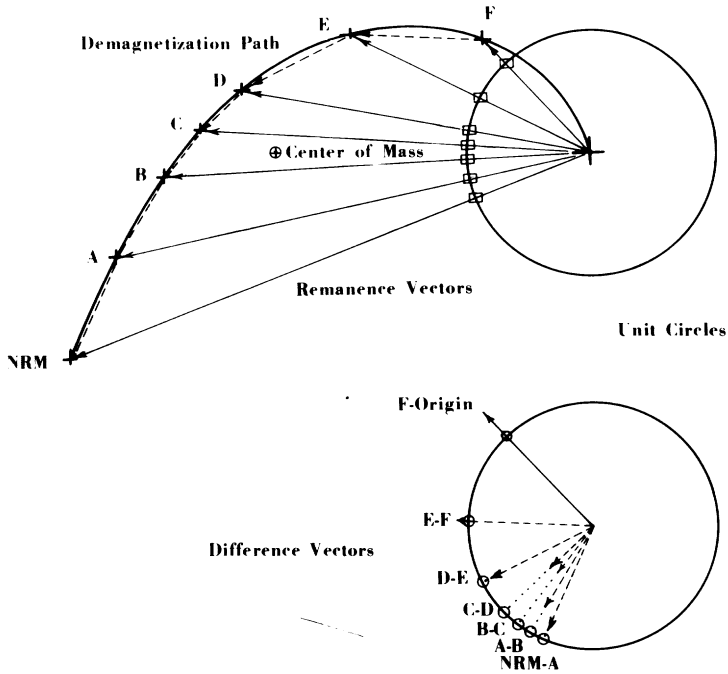
Figure 2. Five methods for estimating the direction of a pole to a set of coplanar points, NRM to origin. Upper diagram: free demagnetization planes pass through the centroid (⊕), while anchored planes are fixed to the origin. Remagnetization circles are fit to unit directions on the sphere and again include the origin. Lower diagram: difference vectors form another group of points to which a plane constrained to include the origin may be fit. Finally, a plane may be fit to the difference vector paths.

points on the unit sphere. This new plane should parallel the old. Note that the normalization step is not necessary; an anchored plane may be fit directly to the difference vectors.

The philosophy underlying the truncation of vectors to unit length is a further difference which should be discussed in the comparison of these techniques. For vector data from a single palaeomagnetic specimen, this step at first seems to be unnecessary. Intensity is as much a part of vectors as is their direction; its omission requires at least some justification. One situation in which truncation might be advantageous is where a component of particular interest is much smaller than the other. Remagnetization circles in this case may discriminate against the strong component, and enhance the relative effect of the smaller one (example 7.1). On difference vector paths, however, vectors of small magnitude have far more scatter in direction due to subtraction errors than do the larger vectors; in this case truncation to unit length clearly worsens the fit. If run without the truncation, a fit of the vector difference plane would weight the vectors according to their intensity and reduce this scattering error. These two types are respectively referred to as 'difference vectors' and 'difference-vector paths', and will be examined further in the first example.

Of these various techniques, only the free demagnetization plane and the vector difference methods can determine the orientation of a plane which does not include the origin; the vector subtraction process in this latter method, however, by itself will increase the scatter in the data and thereby reduce the accuracy of fit. Poles to demagnetization planes can be used in place of those from both remagnetization circles and vector difference paths in the two techniques discussed next.

5.2 SEPARATION OF MULTICOMPONENT NRM: HOFFMAN–DAY DIRECTIONS

Hoffman & Day (1978) recognized that it is sometimes possible to isolate uniquely the direction of a magnetic component which contributes to a demagnetization path even though it may never by itself form a straight line segment. Their original technique used two difference-vector paths from a single specimen which converged (as viewed on a stereonet) at a common direction. Fig. 3 shows how these Hoffman–Day directions may be found using demagnetization planes. The overlap of three components A, B and C is least in row (A), and greatest in row (D), as shown by the stability spectra in the first column of figures. The second column shows the three-dimensional shape of the corresponding demagnetiza- tion path in three-space, and the third plots the difference vector paths one would observe on a stereonet (used by Hoffman & Day). Numerals along each diagram indicate the number of different components simultaneously being removed at that point. Adjacent component pairs which form planes [A, B] and [B, C] in rows (B) to (D) result in two great-circle difference-vector paths which intersect at the direction of component B; thus the direction of B may be found even when it is not uniquely exposed as in rows (C) and (D).

Neighbouring demagnetization planes can be used in place of the difference-vector paths, however, because the intersection line of planes [A, B] and [B, C] on Fig. 3 is parallel to component B. (Two planes intersect along a common line; the common line in this case is B.) This is clear for Fig. 3 (A) where the planes [A, B] and [B, C] are defined by pairs of the three straight line segments. Since corresponding planes in each column of Fig. 3 are parallel (e.g. [A, B] from Fig. 3(A) is parallel to [A, B] from Fig. 3(B), etc.) the direction of B may be recovered even for the example of Fig. 3(D) where there are no linear segments. If $P_{[A, B]}$ and $P_{[B, C]}$ are the respective poles to these demagnetization planes, the direction of B is given by the vector cross product $P_{[A, B]} \times P_{[B, C]}$. In general, if a single palaeomagnetic specimen has K components which overlap as shown in Fig. 3, the direction of K-2 of them may be found with this method. Note that use of demagnetization planes avoids the vector subtraction and intensity truncation steps that increase noise on vector difference paths (see example 7.1).

5.3 INTERSECTING DEMAGNETIZATION PLANES

Situations occasionally arise in palaeomagnetic studies where most specimens share a common magnetic component, but have between them a number of variable, randomly directed overprints. Progressive demagnetization of these specimens then may yield remagnetization circles on a stereonet which tend to converge or diverge from the common direction. Halls (1976, 1977, 1978, see also McFadden 1977) recently discussed least-squares techniques for making estimates of this common direction. Halls first found poles to the remagnetization circles as outlined above, and then repeated the procedure using the poles from all of the specimens. The pole to the final plane was considered to be the best estimate for the direction of the magnetic component common to all samples. Of course, both free and anchored demagnetization planes may be used in place of the remagnetization circles for this type of analysis, thereby increasing the amount of available data.

The final distribution of poles in Halls' analysis cluster about a great circle on the unit sphere. Individually, each pole indicates one direction where the remanence does *not* lie, but taken as a group they reveal by elimination the common direction. Although not discussed by Halls, these data constitute an equatorial or girdle distribution of the type studied and applied to geological problems by Bingham (1964, 1974) and Watson (1960, 1965, 1966). As noted by Onstott (1978; and in press), Bingham's general distribution is applicable
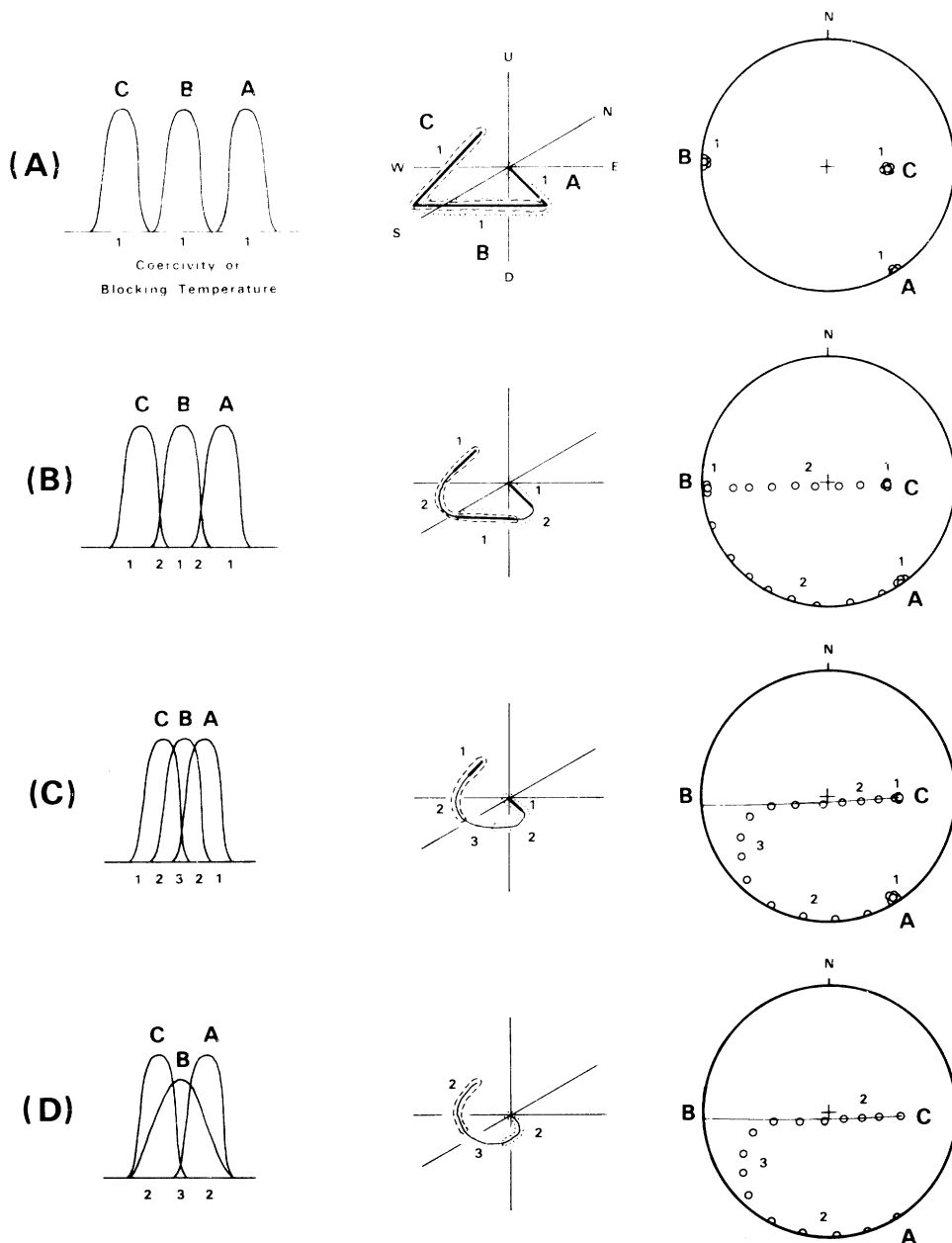
Figure 3. Hoffman—Day directions. In each figure, the letters A, B and C each refer to a separate magnetic component. Small numerals give the number of different magnetic directions being removed simultaneously due to overlap of the coercivity or blocking temperature spectra. Two demagnetization planes are shown in the central figure of each row; the [B, C] plane is enveloped with a dashed line, and dotted line surrounds the points on the [A, B] plane. Dark lines in this figure show linear regions. The stereonet shows the direction of vectors removed sequentially by demagnetization (the difference vector paths), open symbols are on the upper hemisphere. (A) — No overlap in components, all lines and planes may be found. (B) — Slight overlap between neighbours, lines and planes are still present. (C) — Component B completely overlaps A and C, with a slight A—C overlap. No linear part of B remains, but the direction may be found as discussed in the text. (D) — B overlaps completely with A and C, no linear segments remain but the B direction may still be recovered. Figure adapted from Hoffman & Day (1978).

to both bimodal and girdle palaeomagnetic data and may be used to calculate directional concentration parameters and 95 per cent confidence angles about each eigenvector, including the remanence direction.

   Although it is not the purpose of this paper to weigh the relative merits between Fisher's (1953) and Bingham's (1964, 1974) distributions, Bingham statistics will be used here primarily for three reasons: first, it is antipodally symmetric. If L is an observed unit direction of a line or a pole to a plane, $(-L)$ contributes identically to Bingham's analysis. This is necessary because the pole to a demagnetization plane could be chosen in either direction. Secondly, Bingham's distribution equally handles bimodal, girdle and asymmetric girdle data, and is not constrained to circular symmetry. Finally, Bingham statistics are based on a matrix similar to that used in principal component analysis (equation 1). Onstott (1978, and in press) gives a definitive evaluation of this topic in relation to palaeomagnetic studies.

6 Estimation of remanence directions using both lines and planes

As noted earlier, a demagnetization line is an estimate of the direction of a discrete magnetic component, while a pole to a demagnetization plane is an estimate of where the two magnetic components defining it do not lie. Palaeomagnetic studies may identify some specimens with discrete lines while others have secondary overprints and yield only planes. For computing an average remanence direction, one first would like to use data from specimens which had good demagnetization lines, and then further constrain the result by including demagnetization planes from all samples which did not yield good lines. In this manner the best data from each specimen would contribute to the average magnetic direction reported. The proper technique should treat demagnetization lines and Hoffman–Day directions equally and allow for the calculation of error parameters about the final direction. Two methods of attacking this problem are outlined below, although both are as yet incomplete.

6.1 METHOD 1

Viewed as points, data from demagnetization lines and Hoffman–Day directions relating to a common component will group in one or two clusters (normal and reversed polarity) at opposite ends of the unit sphere. On this same sphere, poles to demagnetization planes will distribute themselves about an equator roughly $90°$ from these bipolar clusters. To find a best estimate of the remanence direction, we want to pass a line through the centre of the sphere so that it comes out at either end as close as possible to the bipolar clusters, while being as distant as possible from the poles along the equator. In essence, poles to demagnetization planes are 'repelling' the line while the bipolar points 'attract' it. The mathematical problem becomes that of jointly minimizing the sum of squared deviations from the line to the bipolar data while maximizing the squared deviations from the equatorial points. Maximizing the deviations for the poles, however, is equivalent to minimizing their deviations from a plane which passes through the origin perpendicular to the line (Schomaker *et al.* 1958). Therefore, let D_i, $i = 1, I$ be the distance from the ith demagnetization line or Hoffman–Day direction on the unit sphere to the line through the centre, and let D_j, $j = 1, J$ be the corresponding distance from one of the poles from demagnetization planes to the perpendicular plane. The best remanence direction is then that which minimizes the sum:

$$S = \Sigma D_i^2 + \Sigma D_j^2 \tag{4}$$

Using the method of Lagrange multipliers, one eventually finds the matrix relation:

$$(H_j - H_i - \lambda I)M = 0 \tag{5}$$

where H_j and H_i are the respective matrices of the sums of squares and products for the plane and line data (like equation (1) with $U = [0, 0, 0]$), M is a unit vector, and λ is the Lagrange multiplier. The minimum eigenvector from the combined matrix, $H' = H_j - H_i$, is now the best least-squares estimate of the joint remanence direction. This procedure may be equally used to find the best direction for a sample with many specimens or to combine data from many samples.

Although this procedure will isolate the best remanence direction with both lines and planes, the corresponding problem of calculating the directional (Bingham-type) concentration parameters and error-ovals has not yet fully been solved. The intermediate eigenvector of H' will parallel the largest (least-precise) axis of the confidence oval, and it is known that the eigenvalues of H' sum to $J - I$. Further work on this problem is continuing.

6.2 METHOD 2

If through some simple transformation the equatorial and bipolar groups of points on the unit sphere could be mapped into a common spherical distribution, the data would be homogeneous and manageable. Again, this transformation should treat demagnetization lines and Hoffman–Day directions equally and allow for the calculation of error parameters. One such transformation is to replace each direction in the bipolar cluster with two others which are mutually orthogonal to it. These two new points then lie on the equatorial distribution along with poles from the demagnetization planes, and the final distribution may be handled like those for the intersecting demagnetization planes discussed above. Fortunately, it has been shown that *any* two orthogonal directions considered as a pair in this manner contribute equally to each term in the matrix of sums and squares and products (equation (1) with $U = [0, 0, 0]$). Thus, an arbitrary pair of mutually orthogonal points perpendicular to a line or Hoffman–Day direction may be used in the analysis without loss of generality, and Bingham statistics may be calculated from the final matrix. An unresolved question, however, is the manner in which the two new equatorial points should be weighted in the analysis compared to poles from demagnetization planes. The one-specimen, one-point rule commonly used in Fisherian statistics suggests that the two new directions each be given half weight since they arise from only one specimen. Eigenvalues from the joint matrix will then sum to the total number of samples, N. Therefore, in lieu of a more rigorous derivation, half weights will be used in the following examples.

7 Examples

7.1 NON-INTERSECTING DEMAGNETIZATION PLANES: AN EXAMPLE FROM SIBERIA

For this first example, 126 separately oriented samples were collected from a locality called Zerinsky Mys south of Yakutsk on the Lena River in Siberia (USSR). Oriented cores 2.5 cm in diameter were collected with a hand-held drill at regular intervals from 55 m of red to grey, flat-lying limestone. Strata were palaeontologically dated as lower Tommotian to Atdabanian (both lower Cambrian). One specimen from each core was thermally demagnetized using standard techniques in nine steps up to 650°C (NRM, 150, 250, 350, 450, 500, 530, 560, 610, 650). Of the pale-grey samples, 46 became unstable and gave irreproducible results after treatment above 560°; for these, the unstable steps were omitted

from the subsequent analysis as they clearly did not represent measurements of the natural magnetism. Presumably, their remanence was carried by magnetite and/or titanomagnetite with Curie temperatures near 580°C. The magnetization of these rocks will be described in more detail elsewhere (Kirschvink & Rozanov, in preparation).

The natural remanent magnetization (NRM) for most of the Siberian rocks was directed northerly with steep downward inclination, suggesting that most of it was recently acquired in the present magnetic field. Upon progressive demagnetization, 96 samples produced visually acceptable arcs on a stereonet and indicated the presence of a two-polarity component of smaller magnitude and higher thermal stability. Only three specimens reached stable endpoints. The two-component system present in 96 specimens therefore offers a good test for comparing various techniques which have been proposed for estimating the orientation of coplanar points along a demagnetization path.

As noted earlier, either of two antiparallel directions may be used to specify the direction for a pole to a demagnetization plane without affecting Bingham statistics. The direction in which the remanence moves upon demagnetization may have significance for polarity interpretation, however, so it seems advantageous to consistently select one of the directions. In the example at hand, most arcs begin at steep, northerly directions and move upon demagnetization towards shallow NE or SW declinations, depending upon the polarity of the primary (more stable) component. For this and in the following examples, a right-handed convention has been used for selecting the pole direction (e.g. the pole most parallel to the vector cross-product, (low demag) × (high demag), represents the plane). Thus poles with SE declinations indicate arcs moving towards the NE, and NW declinations indicate arcs moving toward the SW.

In the present example, tectonic or other geologic processes have not acted to scatter one magnetic component relative to the other. This case is therefore distinctly different from those described by Halls (1976, 1978) where both discrete directions could be found by using converging circular paths. These are sub-parallel, non-converging remagnetization paths. In the converging case, the scatter of one component relative to the other will cause poles to demagnetization planes to distribute themselves about an equator on the unit sphere. Poles will still lie on an equator if neither component is scattered, however, but they will tend to fall in two clusters at opposite ends of the unit sphere. This is a girdle distribution with high circular asymmetry (Bingham 1974), and as such resembles the bipolar cluster of line data. These clusters are perpendicular to both magnetic components; the principal eigenvector from the spherical least-squares calculation gives the best estimate of where neither magnetic component lies. Although this information would not tell the direction of the primary component, it locates a plane in which it must lie. The orientation of this plane may then be used to constrain the palaeogeographic position of the continent involved.

Each of the five different methods discussed earlier were used to estimate the directions of poles to the 96 Siberian demagnetization planes. Stereographic equal-area projections on Fig. 4 give these directions in order of increasing complexity, going from free demagnetization planes (Fig. 4A), anchored demagnetization planes (Fig. 4B), remagnetization circles (Fig. 4C, Halls 1976), difference vectors (Fig. 4D), and to difference-vector paths (Fig. 4E, Hoffman & Day 1978). Table 1 lists the principal eigenvector for each set of data, along with the two Bingham concentration parameters and 95 per cent angles of confidence about it. Visual inspection of Fig. 4(A–E) reveals that in each case the poles are distributed along a great circle which dips to the SE, with two somewhat dense clusters in the NW and SE. Values for $K2$ in Table 1 would be near 0 if the data were circularly distributed about the equator, thus the observed $K2$ values indicate a moderate tendency for circular asymmetry.
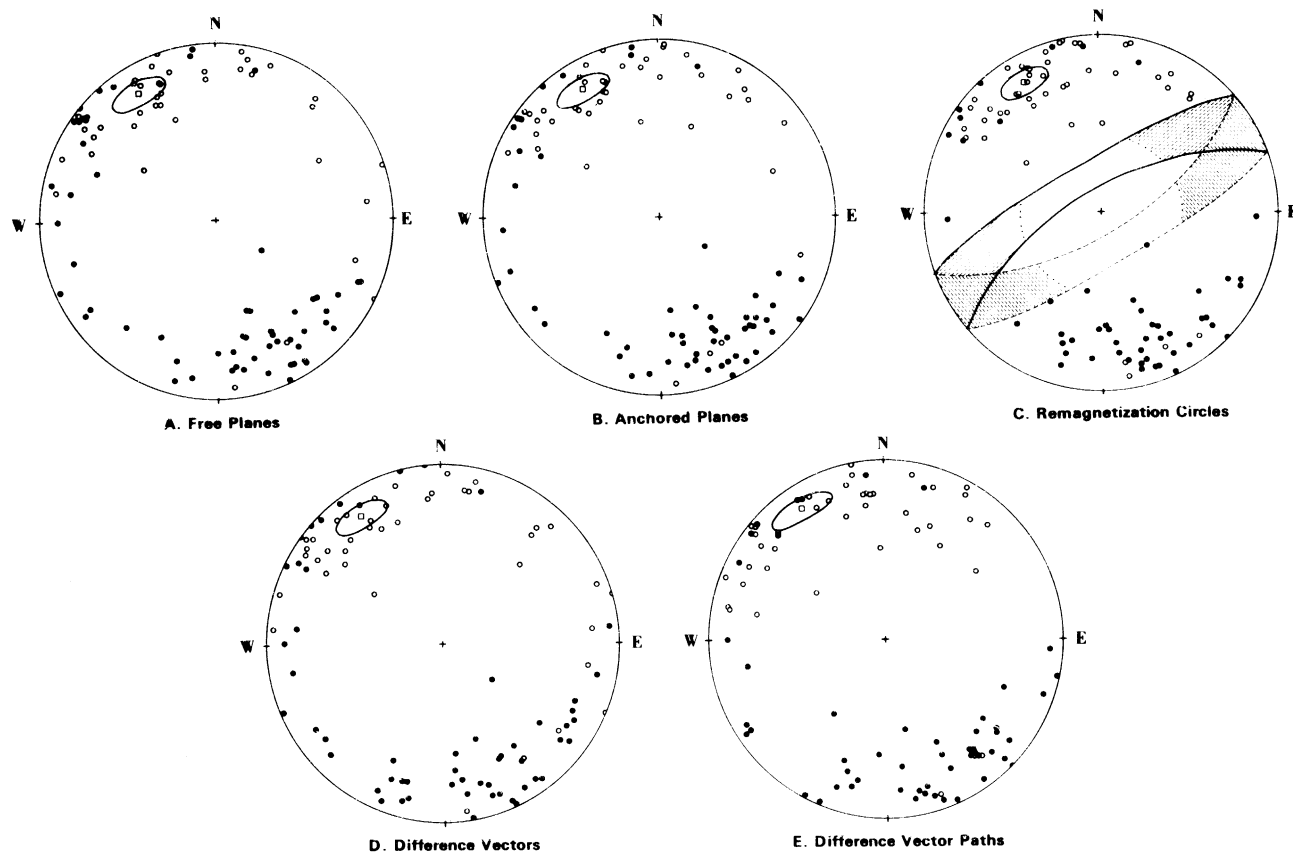
Figure 4. Comparison of pole directions for coplanar demagnetization data obtained with each of the five methods outlined on Fig. 2. Original magnetic data come from 96 Siberian samples collected at Zerinsky Mys. Open symbols indicate directions on the upper hemisphere (negative inclination). Open squares show the direction of the principal eigenvectors from the restricted data set (MAD < 15°) along with their ovals of 95 per cent confidence. (C) also gives the 95 per cent boundaries along a girdle distribution in which both the primary and secondary magnetic directions lie; the shaded portion of the girdle corresponds to palaeoinclinations below 30° north or south.

Table 1. Comparison of planar techniques for non-intersecting Siberian demagnetization planes.

All planes:	N	u_1 Dec	u_1 Inc	$K1$	$K2$	ov. az.	$\alpha_{95\,min}$	$\alpha_{95\,max}$
Free planes	96	330.9	−16.3	−9.3	−2.4	103.8	4.1	9.7
Anchored planes	96	335.1	−16.9	−8.6	−2.7	103.4	4.3	8.7
Remagnetization circles	96	338.2	−17.7	−8.2	−3.6	103.5	4.2	7.0
Difference vectors	96	329.8	−15.2	−10.3	−1.8	101.9	4.0	12.6
Difference vector paths	96	336.1	−16.6	−10.1	−2.1	99.7	4.0	10.6
Planes with MAD < 15°:								
Free planes	37	328.8	−16.9	−8.7	−3.6	95.1	6.6	11.1
Anchored planes	37	329.6	−17.3	−8.6	−3.6	94.4	6.6	11.0
Remagnetization circles	37	329.6	−16.8	−8.2	−4.1	92.4	6.7	10.1
Difference vectors	37	327.5	−16.6	−8.8	−3.8	96.1	6.5	10.8
Difference vector paths	37	327.3	−14.3	−9.9	−3.1	98.3	6.1	12.6

N – Number of specimens contributing demagnetization planes to the analysis.
u_1 – (Dec, Inc) Direction of the principal eigenvector. For this analysis, u_1 estimates the direction in which neither magnetic component lies.
ov. az. – The spherical angle measured at u_1 between vertical and u_2. Directions for the two eigenvectors unspecified in this table (u_2 and u_3) may be found using the direction of u_1 and the ov. az.
$K1$, $K2$ – Bingham's concentration parameters (from density $d^{-1}[K1, K2]\exp[K1(u_3 \cdot L)^2 + K2(u_2 \cdot L)^2]$, where L is the random population variable, and d^{-1} is a normalizing constant).
$\alpha_{95\,min}$, $\alpha_{95\,max}$ – Bingham's (1974) approximate angles of 95 per cent confidence. The direction of $\alpha_{95\,max}$ always parallels the intermediate eigenvector (u_2).

Similarly, directions for the principal eigenvector (u_1) found with each of the five methods do not vary significantly.

Closer examination, however, reveals that the direction of a pole to coplanar data from a single specimen may vary greatly depending upon which technique is used. For example, the bipolar cluster for the remagnetization circles on Fig. 4(C) is more distinct than those on any of the other diagrams; apparently removing the intensity data in this case slightly improves resolution of the primary component. A more direct test is to compare the angular difference between estimates of the poles for each specimen with the general coplanarity of the data. The histogram on Fig. 5(A) shows the distribution of specimens versus their coplanarity measured by the maximum angle of deviation (MAD, equation 3 above). The Siberian samples clearly have a wide spectrum of coplanarity; 37 specimens have deviation angles of less than 15°, while 21 have angles greater than 25°. Intuitively, one expects highly coplanar data to yield essentially the same pole direction regardless of the technique used, while marginally coplanar data would yield wildly different directions. Scatter diagrams (Fig. 5B–E) test this prediction by comparing the maximum angle of deviation (MAD) against the angular distance between poles. Each point on these diagrams represent one specimen; points to the left represent highly coplanar data while points to the right do not. If every technique gave identical results, all points on these scatter diagrams would lie close to the horizontal axis. Fig. 5(B and D) show that there is good directional agreement between free planes, anchored planes, and difference vectors for MAD values below 15°. Above this, however, angular differences of nearly 90° are found. The comparison between free planes, remagnetization circles, and difference-vector paths (Fig. 5C and E) is far worse – angular differences of 45° or more occur from specimens with small MAD values. Below values of 15°, remagnetization circles fare slightly better than difference-vector paths; eight
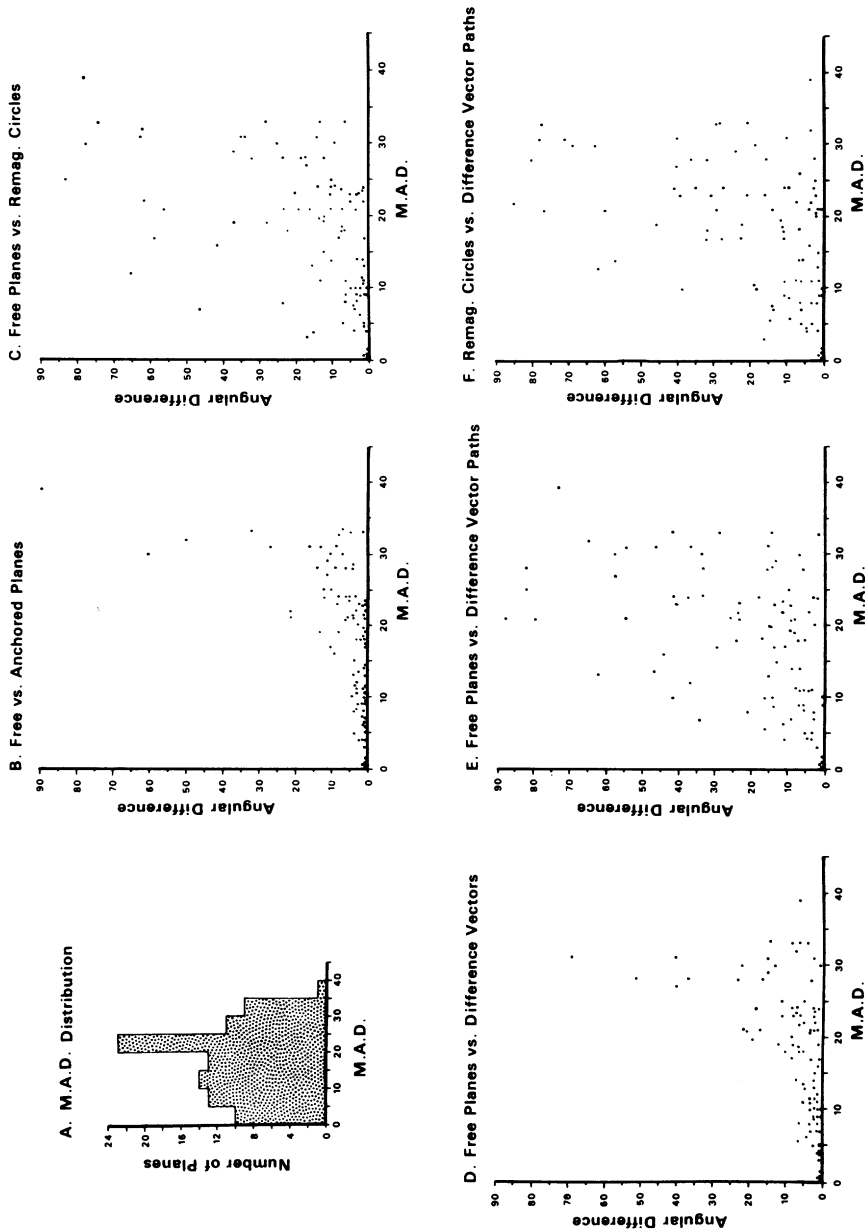
Figure 5. Comparison of planar techniques. (A) – Distribution of MAD values for 96 Siberian samples. (B) to (F) – Scatter diagrams showing agreement of pole directions versus coplanarity of points.

of 37 circles change their direction by more than $10°$ whereas 14 of 37 difference-vector paths change. Truncation of the intensity is probably responsible for these differences when compared to free demagnetization planes. A similar comparison between remagnetization circles and difference-vector paths (Fig. 5F) shows poor directional agreement.

In summary, difference vectors, free and anchored demagnetization planes yield similar poles to coplanar demagnetization data for MAD values below $15°$; remagnetization circles enhance the effect of weak components while difference-vector paths increase the degree of scatter. Because pole directions were not highly reproducible for the 59 samples with MAD values larger than $15°$, they were removed and the calculations for Table 1 repeated as
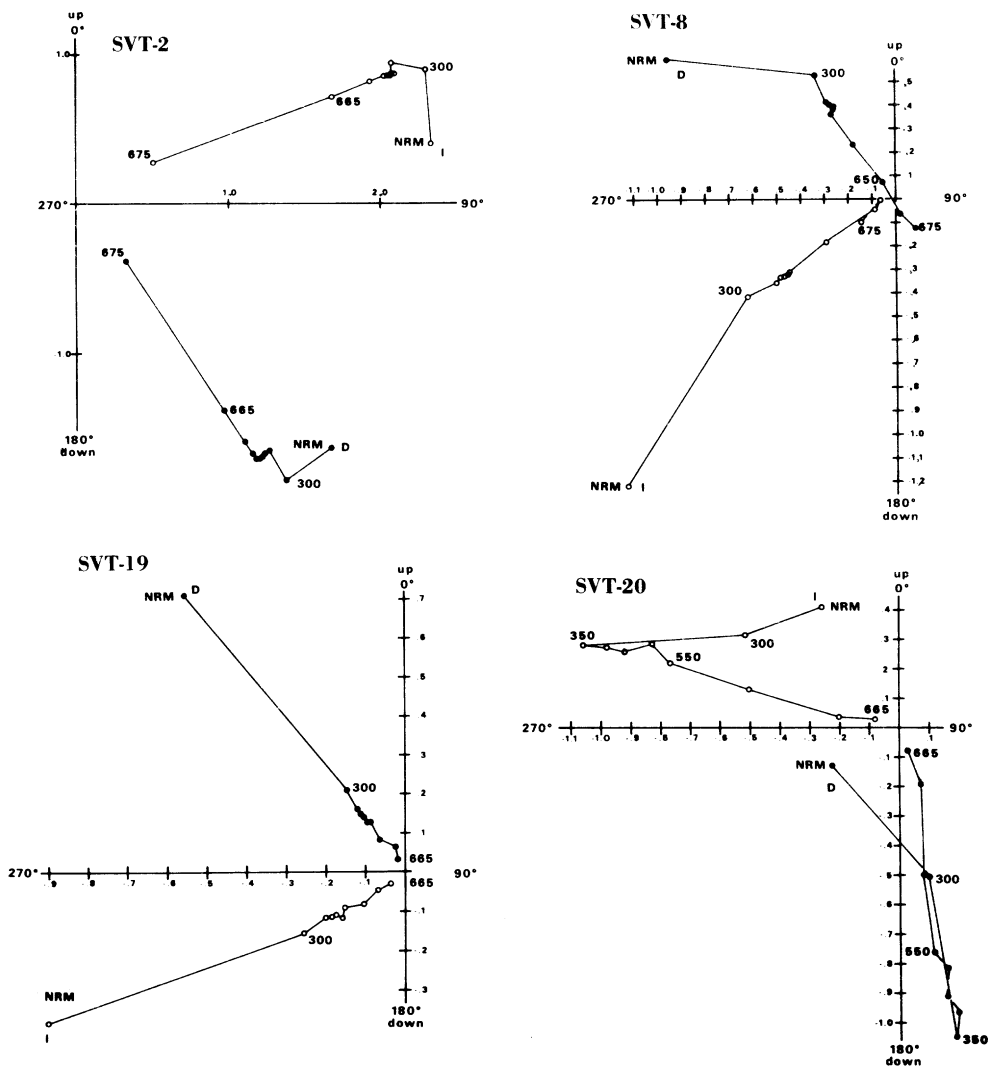
Figure 6. Vector demagnetization diagrams. Numbers along the axes refer to the magnetic intensity in units of 10^{-6} emu g^{-1} (or A m^2 kg^{-1}). Paths labelled D (declination) show the horizontal projection into the bedding plane of the demagnetization path, and those labelled I (inclination) plot the vertical component against the horizontal. Although it is not strictly an orthogonal projection, an inclination curve plotted in this fashion directly shows the inclination and intensity of the remanence vector at each demagnetization point. Occasionally, a line will plot on this curve as part of a hyperbola. The sampling locality, Tiout, is at $30.35°$ N, $8.67°$ W.

shown. In each case the value of $K2$ became more negative indicating a greater tendency for bipolar clustering. Again, the direction for u_1 is not sensitive to the particular technique used. For the remaining 37 samples, Bingham's (1974) asymptotic ovals of 95 per cent confidence around the principal eigenvector are shown on each diagram on Fig. 4. With 95 per cent confidence, the primary remanence direction should lie somewhere within the equatorial bands drawn on Fig. 4(C). Given the additional geologic information that there are diverse Archeocyathid bioherms with abundant carbonate sediments, a low-latitude of deposition ($\leqslant 30°$) may be inferred. The shaded area on Fig. 4(C) therefore gives the most probable locus of the palaeomagnetic axial dipole direction for Lower Cambrian time on the Siberian platform. This is as far as the analysis of the primary magnetic component may go without invoking additional assumptions concerning the nature of the blocking temperature distribution for each component.

7.2 JOINT LINE AND PLANE ANALYSIS: THE SÉRIE LIE DE VIN, MOROCCO

In the previous example, remagnetization parallel to the present local magnetic field obscured the primary magnetic component of most specimens. A better example to illustrate the joint analysis of demagnetization lines and planes comes from the basal units of the Late Precambrian Série lie de Vin, exposed near the village of Tiout in the Anti—Atlas mountains, Morocco. A total of 28, 2.5 cm diameter oriented core samples were collected at regular intervals through 70 m of strata. One specimen from each core was subsequently thermally demagnetized in a manner similar to that described for the Siberian samples above. Typical demagnetization paths are shown on the vector diagrams in Fig. 6. Above 300—350°C, most specimens decay linearly towards the origin and indicate the presence of a single characteristic magnetic component. A principal component search of the data set along the lines of Fig. 1 located 21 specimens, each of which had four or more collinear points and MAD values of less than $10°$. Of these, 19 included the origin. Although the remaining seven specimens did not have demagnetization lines, all had demagnetization planes with five or more points and MAD values below $10°$. Corresponding directions for lines and planes of best least-squares fit, anchored to the origin where appropriate, are shown in Fig. 7(A).
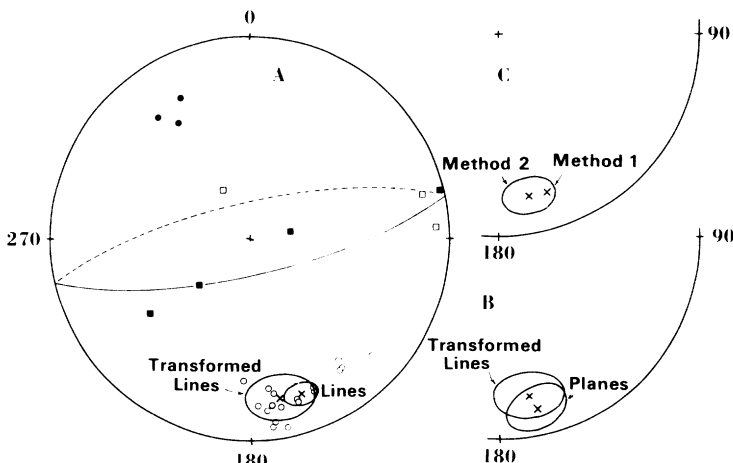

Figure 7. Results from the Série lie de Vin, Morocco. (A) — Circles are the directions for 21 demagnetization lines with MAD values below $10°$. Squares show similar directions to the poles for the remaining seven demagnetization planes. Ovals plotted on A, B and C are the average directions and Bingham 95 per cent confidence ovals as listed on Table 2.

Table 2. Combined line and plane directions for the Série lie de Vin, Anti–Atlas Mountains, Morocco. Results enclosed with parentheses have not been corrected for local tilt of the strata.

	N	Dec	Inc	K1	K2	ov. az.	$\alpha_{95\,min}$	$\alpha_{95\,max}$
Lines	(21	168.1	−38.7	−26.25	−10.03	118.3	4.4	7.3)
	21	161.8	−20.2	−17.36	−14.44	105.4	5.4	6.0
Lines, transformed	(21	175.9	−39.4	−11.10	−0.41	127.7	9.4	10.7)
	21	169.4	−21.2	−8.82	−0.32	113.7	10.9	12.1
Planes	(7	175.8	−36.1	−70.41	−0.82	42.8	5.8	7.2)
	7	167.6	−14.5	−28.46	−0.94	35.2	9.2	11.9
Method 1 combined	(28	169.5	−38.2			48.8		
	28	162.9	−19.3			47.3		
Method 2 combined	(28	176.1	−38.5	−13.16	−0.05	116.1	7.6	7.9)
	28	169.3	−19.7	−10.05	−0.10	70.0	8.6	9.2

N – Number of lines or planes in each analysis.
Dec, Inc – Direction of average remanence.
$K1, K2$ – Bingham concentration parameters (see Table 1).
ov. az. – The spherical angle measured at the remanence direction between vertical and the direction of $\alpha_{95\,max}$.
$\alpha_{95\,min}$, $\alpha_{95\,max}$ – Bingham's (1974) approximate angles of 95 per cent confidence. The direction of $\alpha_{95\,max}$ always parallels the intermediate eigenvector.

As expected, poles to the seven demagnetization planes lie on a great circle roughly 90° from the antipodal cluster of linear directions.

Table 1 and Fig. 7 separately list and plot the remanence directions and associated Bingham statistics for the collinear and coplanar data, as well as for the equatorially transformed lines (Section 6.2 above) and joint estimates (methods 1 and 2, Sections 6.1 and 6.2 above). After tilt correction, the remanence direction as estimated separately from lines and planes differs by 8°, it is therefore worthwhile to test the hypothesis that the directions are not statistically different before the data are used in a joint calculation. At the present time, the best available method for doing this is to transform the antipodal line directions into a girdle distribution according to Section 6.2 above, and then use Watson's (1965) directional test. Written in terms of the eigenvalues, large values of the F-ratio statistic,

$$F_{(2, L+P-4)} = \frac{L+P-4}{2} \cdot \frac{\lambda_{min,\,combined} - \lambda_{min,\,planes} - \lambda_{min,\,T.\,lines}}{\lambda_{min,\,planes} + \lambda_{min,\,T.\,lines}} \qquad (6)$$

indicate that the directions are distinct. For this example with 21 lines and seven planes, $F_{2,\,24} = 0.278$, implying that the directions cannot be distinguished at the 99 per cent confidence level and they may be combined. Note, however, that the equatorial transformation of the linear data alone produced a 7° shift in remanence direction which may have contributed to the apparent significance of this test. The combined remanence direction found with method 2 also reflects this bias and is closer to the transformed line directions than the original. Method 1 yields the preferred remanence direction which lies between that computed for isolated lines and planes, but error parameters cannot, as yet, be calculated for it.

Conclusions

1. Principal component analysis may be used to find and estimate the directions of lines and planes of best least-squares fit along a demagnetization path of a palaeomagnetic specimen.

These lines and planes are based on all of the available data, not just on the two end points of a line segment (like vector subtraction) or on directions devoid of intensity (like remagnetization circles and difference vector paths).

2. Because eigenvalues from the principal component analysis are the variance (σ^2) around the mean along each principal axis, they may be used to indicate the relative collinearity or coplanarity of a set of points. The Maximum Angular Deviation (MAD) calculated from the variance provides a palaeomagnetic precision index based only on the geometry of the data set.

3. Demagnetization planes may be used in place of difference-vector paths for locating Hoffman—Day directions, thereby increasing the accuracy by avoiding the vector subtraction and intensity truncation steps.

4. Demagnetization planes are useful in palaeomagnetic studies because their poles give an estimate of a direction in which two magnetic components do not lie. This additional information may be used along with directions from demagnetization lines to estimate an average direction for a component of magnetic remanence.

Acknowledgments

References

Ade-Hall, J. M., 1969. Opaque petrology and the stability of natural remanent magnetism in Basaltic rocks, *Geophys. J. R. astr. Soc.,* 18, 93—107.

Andel, J., 1970. Negative analysis of the stability index, *Studia geophys. geod.,* 14, 310—324.

Bingham, C., 1964. Distributions on the sphere and on the projective plane, *PhD dissertation,* Yale University.

Bingham, C., 1974. An antipodally symmetric distribution on the sphere, *Ann. Statist.,* 2, 1201—1225.

Blow, D. M., 1960. To fit a plane to a set of points by least-squares, *Acta crystal.,* 13, 168.

Briden, J. C., 1972. A stability index of remanent magnetism, *J. geophys. Res.,* 77, 1401—1405.

Collinson, K. M., Creer, K. M. & Runcorn, S. K., eds, 1967. *Methods in Paleomagnetism,* Elsevier, Amsterdam.

Creer, K. M., 1957. The remanent magnetization of unstable keuper marls, *Phil. Trans. R. Soc. A,* 250, 130—143.

Creer, K. M., 1962. A statistical enquiry into the partial remagnetization of folded Old Red Sandstone Rocks, *J. geophys. Res.,* 67, 1899—1906.

Dimroth, E., 1963. Fortschritte der Gefugestatistik, *N. Jahrbuch Mineral.,* 186—192.

Fisher, R. A., 1953. Dispersion on a sphere, *Proc. R. Soc. Ser. A.,* 217, 295—305.

Frankel, R. B., Blakemore, R. P. & Wolfe, R. S., 1979. Magnetite in freshwater magnetic bacteria, *Science,* 203, 1355—1356.

Goree, W. S. & Fuller, M., 1976. Magnetometers using RF-driven squids and their applications in rock magnetism and palaeomagnetism, *Rev. Geophys. Space Phys.,* 14, 591.

Halls, H. C., 1976. A least-squares method to find a remanence direction from converging remagnetization circles, *Geophys. J. R. astr. Soc.,* 45, 297—304.

Halls, H. C., 1977. Reply to P. L. McFadden's comments, *Geophys. J. R. astr. Soc.,* 48, 551–552.

Halls, H. C., 1978. The use of converging remagnetization circles in paleomagnetism, *Phys. Earth planet. Interiors,* 16, 1–11.

Hoffman, K. A. & Day, R., 1978. Separation of multi-component NRM: a general method, *Earth planet. Sci. Lett.,* 40, 433–438.

Hotelling, H., 1933. Analysis of a complex of statistical variables into principal components, *J. educ. Psychol.,* 24, 417–441, 498–520.

Khramov, A. N., 1958. In *Paleomagnetism and its Application to Geological and Geophysical Problems,* p. 75, ed. Irving, E., Wiley, New York.

Kirschvink, J. L. & Lowenstam, H. A., 1979. Mineralization and magnetization of chiton teeth: paleomagnetic, sedimentologic, and biologic implications of organic magnetite, *Earth planet. Sci. Lett.,* 44, 193–204.

Lund, S. P. & Strelitz, R. A., 1979. Uncertainties in principal value components analysis of paleomagnetic poles, *Trans. Am. Geophys. Un.,* 60, 818.

McFadden, P. L., 1977. Comments on 'a least-squares method to find a remanence direction from converging remagnetization circles' by H. C. Halls, *Geophys. J. R. astr. Soc.,* 48, 549–550.

Molyneux, L., 1971. A complete result magnetometer for measuring the remanent magnetization of rocks, *Geophys. J. R. astr. Soc.,* 24, 429–433.

Onstott, T. C., 1978. Statistical analysis of Nonfisherian distributions: application to paleomagnetics, *Trans. Am. Geophys. Un.,* 59, 1060.

Pearson, K., 1901. On lines and planes of closest fit to systems of points in space, *Phil. Mag.,* 2, 559–572.

Schomaker, V., Wasser, J., Marsh, R. E. & Bergman, G., 1959. To fit a plane or a line to a set of points by least squares, *Acta crystal.,* 12, 600–604.

Stupavsky, M. & Symons, D. T. A., 1978. Separation of magnetic components from af step demagnetization data by least-squares computer methods, *J. geophys. Res.,* 83, 4925–4932.

Symons, D. T. A. & Stupvasky, M., 1974. A rational paleomagnetic stability index, *J. geophys. Res.,* 79, 1718–1720.

Tarling, D. H. & Symons, D. T. A., 1967. A stability index of remanence in palaeomagnetism, *Geophys. J. R. astr. Soc.,* 12, 443–448.

Watson, G. S., 1960. More significant tests on the sphere, *Biometrika,* 47, 87–91.

Watson, G. S., 1965. Equatorial distributions on a sphere, *Biometrika,* 52, 193.

Watson, G. S., 1966. The statistics of orientation data, *J. geol.,* 74, 786–797.

Zijderveld, J. D. A., 1967. A.C. demagnetization in rocks: analysis of results, in *Methods in Paleomagnetism,* pp. 254–286, eds Collinson, Creer & Runcorn, Elsevier, New York.